

## RESEARCH ARTICLE

# Unr defines a novel class of nucleoplasmic reticulum involved in mRNA translation

Frédéric Saltel<sup>1,2,\*</sup>, Alban Giese<sup>1,2,\*</sup>, Lamia Azzi<sup>1,2,3,\*</sup>, Habiba Elatmani<sup>1,2</sup>, Pierre Costet<sup>4</sup>, Zakaria Ezzoukhy<sup>1,2,†</sup>, Nathalie Dugot-Senant<sup>2</sup>, Lucile Miquerol<sup>5</sup>, Oréda Boussadia<sup>6</sup>, Harald Wodrich<sup>2,7</sup>, Pierre Dubus<sup>1,2,3,#</sup> and Hélène Jacquemin-Sablon<sup>1,2,#,§</sup>

## ABSTRACT

Unr (officially known as CSDE1) is a cytoplasmic RNA-binding protein with roles in the regulation of mRNA stability and translation. In this study, we identified a novel function for Unr, which acts as a positive regulator of placental development. Unr expression studies in the developing placenta revealed the presence of Unr-rich foci that are apparently located in the nuclei of trophoblast giant cells (TGCs). We determined that what we initially thought to be foci, were actually cross sections of a network of double-wall nuclear membrane invaginations that contain a cytoplasmic core related to the nucleoplasmic reticulum (NR). We named them, accordingly, Unr-NRs. Unr-NRs constitute a novel type of NR because they contain high levels of poly(A) RNA and translation factors, and are sites of active translation. In murine tissues, Unr-NRs are only found in two polyploid cell types, in TGCs and hepatocytes. *In vitro*, their formation is linked to stress and polyploidy because, in three cancer cell lines, cytotoxic drugs that are known to promote polyploidization induce their formation. Finally, we show that Unr is required *in vivo* for the formation of Unr-containing NRs because these structures are absent in *Unr*-null TGCs.

**KEY WORDS:** Unr, CSDE1, Polyploid cells, Nucleoplasmic reticulum, mRNA translation, *Unr* knockout

## INTRODUCTION

*Csde1* (cold shock domain-containing E1, also known as and, hereafter referred to as *Unr*), was identified as a transcription unit located immediately upstream of *N-ras* in the genome of several mammalian species (Jeffers et al., 1990; Nicolaiew et al., 1991). Unr is a member of the family of proteins that contain an evolutionarily conserved nucleic-acid-binding domain termed cold-shock domain (CSD). This domain binds single-stranded DNA and RNA (Graumann and Marahiel, 1998), and CSD-containing proteins are involved in transcriptional and/or post-transcriptional control of

gene expression (Mihailovich et al., 2010; Wolffe, 1994). The mammalian Unr proteins, composed of five CSDs, are highly similar by sharing >90% amino acid identity. Unr is a cytoplasmic RNA-binding protein that, *in vitro*, interacts preferentially with purine-rich motifs located in RNA loops (Jacquemin-Sablon et al., 1994; Triqueneaux et al., 1999). Unr has been characterized as a regulator of mRNA turnover (Grosset et al., 2000) and translation. During translation, Unr acts as a positive or negative regulator of specific transcripts; it either stimulates or represses the translation driven by internal ribosome entry sites (IRESs) (Boussadia et al., 2003; Dormoy-Raclet et al., 2005; Hunt et al., 1999; Mitchell et al., 2003) or represses cap-dependent translation (Abaza et al., 2006; Duncan et al., 2006; Patel et al., 2005). Recent studies have identified numerous direct Unr mRNA targets in *Drosophila* (Mihailovich et al., 2010) and in human melanoma (Wurth et al., 2016). In melanoma Unr regulates its specific target genes mainly at the level of translation elongation or termination (Wurth et al., 2016).

Genetic and biochemical studies have linked Unr to several cellular processes as well as to human diseases. Unr has been implicated in the control of cell death (Dormoy-Raclet et al., 2007), cell differentiation (Elatmani et al., 2011) and cell migration (Kobayashi et al., 2013). In humans, recent studies identified important roles for Unr in the promotion of melanoma cell invasion and metastasis (Wurth et al., 2016), as well as in disorders, such as autism or Diamond-Blackfan anemia (Sanders et al., 2012; Xia et al., 2014; Horos and von Lindern, 2012). Unr has also been characterized as being a critical regulator of embryonic development. In *Drosophila*, Unr inhibits dosage compensation in female flies, and Unr overexpression results in predominant male lethality at the larvae stage (Patalano et al., 2009).

Here, we report that Unr is crucial for mouse embryonic and placental development. We also identify an Unr-rich structure, forming a network of cytoplasmic invaginations into the nucleus, reminiscent of the nucleoplasmic reticulum (NR) (reviewed in Malhas et al., 2011). These so-called Unr-NRs, found in polyploid cells, constitute a novel type of NR and are found in polyploid cells, in which active translation takes place.

## RESULTS

### Disruption of the *Unr* gene in mice causes placental defects that coincide with embryonic lethality occurring at mid-gestation

We have previously generated mice carrying an inactivated *Unr* allele as a result of the deletion of the *Unr* promoter and reported that the homozygous mutation of the *Unr* gene results in a null mutation (Boussadia et al., 2003). The lack of Unr protein led to embryonic lethality at mid-gestation, since the percentage of *Unr*<sup>-/-</sup> mutant embryos was detected close to the expected Mendelian levels at 9.5 days of gestation (24%), but were less by day 10.5


<sup>1</sup>INSERM UMR1053 Bordeaux Research In Translational Oncology, BaRITOn, F-33000 Bordeaux, France. <sup>2</sup>University of Bordeaux, F-33000 Bordeaux, France.

<sup>3</sup>Department of Tumor Biology, CHU, F-33000 Bordeaux, France. <sup>4</sup>Laboratoire de Transgénèse, Université Bordeaux, F-33000 Bordeaux, France. <sup>5</sup>Aix-Marseille University, CNRS, IBDM UMR 7288, Marseille, France. <sup>6</sup>Taconic Europe, Centre d'Affaires DMCI, Lyon, France. <sup>7</sup>MFP CNRS UMR 5234, Microbiologie Fondamentale et Pathogénicité, Université de Bordeaux, F-33000 Bordeaux, France.

<sup>†</sup>Present address: Université Mohammed 6 des Sciences de la Santé (UM6SS), Faculté de Médecine, Laboratoire National de Référence (LNR), Casablanca, Morocco.

<sup>#</sup>These authors contributed equally to this work.

<sup>§</sup>Authors for correspondence (frederic.saltel@inserm.fr; helene.jacquemin-sablon@u-bordeaux.fr)

 F.S., 0000-0002-0724-9680

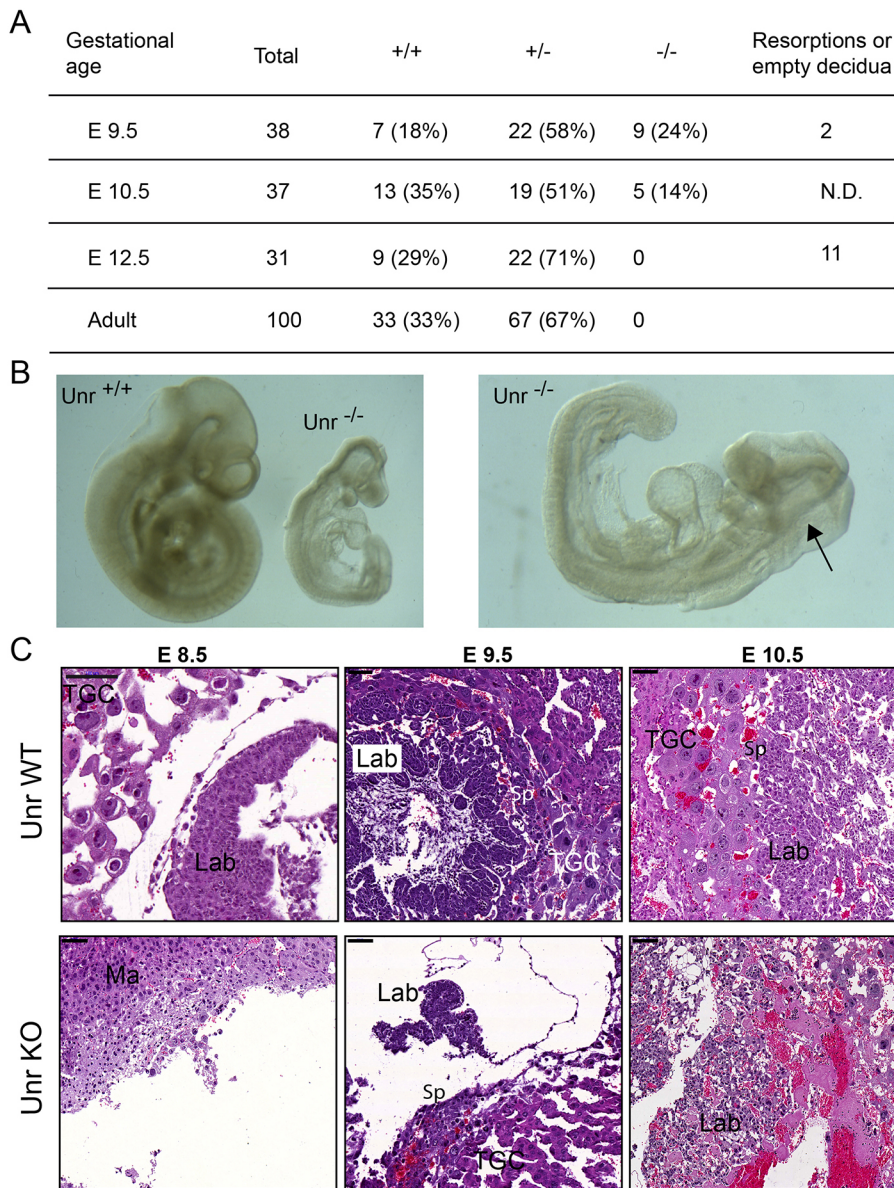


**Fig. 1. *Unr* disruption causes embryonic and placental abnormal development.** (A) Genotype analysis of progeny from *Unr*<sup>+/-</sup> intercrosses. The genotypes of the embryos were determined by PCR using DNA extracted from the whole embryo or from the yolk sac, using primers a, b, c and d as shown in Fig. S1B. In parentheses appear the percentages corresponding to the different genotype classes. N.D., genotype not determined. (B) Morphological defects in *Unr*<sup>-/-</sup> embryos at E9.5. Micrographs of *Unr*<sup>-/-</sup> embryos and control littermates at E9.5 are shown. Note the marked reduction in size of the mutant (right) relative to the control littermate (left) and the absence of neural tube closure (right, the unclosed head is indicated by the arrow). (C) Placental defects in *Unr*<sup>-/-</sup> embryos. Histological analysis of placentas of wild-type and *Unr* KO mice at E8.5, E9.5 and E10.5. Sections through the central regions of placentas were (H&E) stained and imaged at 40 $\times$ . Maternal deciduas (Ma), Spongiotrophoblast (Sp), trophoblast giant cell (TGC), and Labyrinth (Lab) layers are indicated.

(14%) and absent at 12.5 days of gestation and later (Fig. 1A). *Unr*<sup>-/-</sup> embryos were indistinguishable from normal littermates at E7.5. Between E8.5 and E10.5, mutant embryos could be identified morphologically as they are smaller, present delayed growth and, at E9.5–E10.5, lack neural tube closure (Fig. 1B). Heart maturation was delayed in *Unr*<sup>-/-</sup> embryos, which presented a defect of ventricular trabeculation and smaller than normal atrioventricular cushions at the atrioventricular canal (Fig. S1A). The heart was, however, not critically abnormal.

Malfunions of extra-embryonic tissues are primary the cause of embryonic lethality at mid-gestation (Copp, 1995; Ihle, 2000; Rossant and Cross, 2001). Histological analyses of the yolk sac from *Unr*<sup>-/-</sup> mice did not reveal obvious structural changes at E8.5 or later (Fig. S1B). In contrast, at E9.5–E11.5 obvious placental defects were detected in placentas of *Unr* KO mice, when compared to wild-type littermates. The murine placenta consists of maternal and embryonic parts, with the latter being composed of three distinct trophoblastic cell layers; namely, an outermost layer of trophoblast giant cells (TGCs), an intermediate spongiotrophoblast layer and the innermost labyrinthine layer. In placentas of *Unr* KO mice there was a marked atrophy of the

spongiotrophoblast and labyrinthine layers, and an ~60–75% decrease in the number of TGCs (Fig. 1C). These results show that *Unr* is essential for placental development between E8.5 and E11.5.

#### Identification of an *Unr*-rich NR in placental TGCs

We examined the expression of *Unr* protein within wild-type placenta at day 10.5. Immunofluorescence analyses of placental sections revealed that *Unr* is distributed throughout the cytoplasm of the three trophoblastic sub-populations (Fig. 2A, left panel). The specificity of the *Unr* antibody used in this study was shown by the absence of *Unr* staining in immunofluorescence analyses of placentas of *Unr* KO mice (Fig. 2B). In addition, we found that *Unr* also localized to distinguishable foci within the nuclei of a subset of TGCs, but not of spongiotrophoblasts (Fig. 2A, see magnified images of boxed areas). This finding was unexpected because no nuclear expression of *Unr* has been reported so far, prompting us to further characterize these *Unr* foci through physiological, molecular and functional analyses.

First, we performed, by immunohistochemistry, a temporal analysis of the presence of *Unr* foci in TGCs. The results

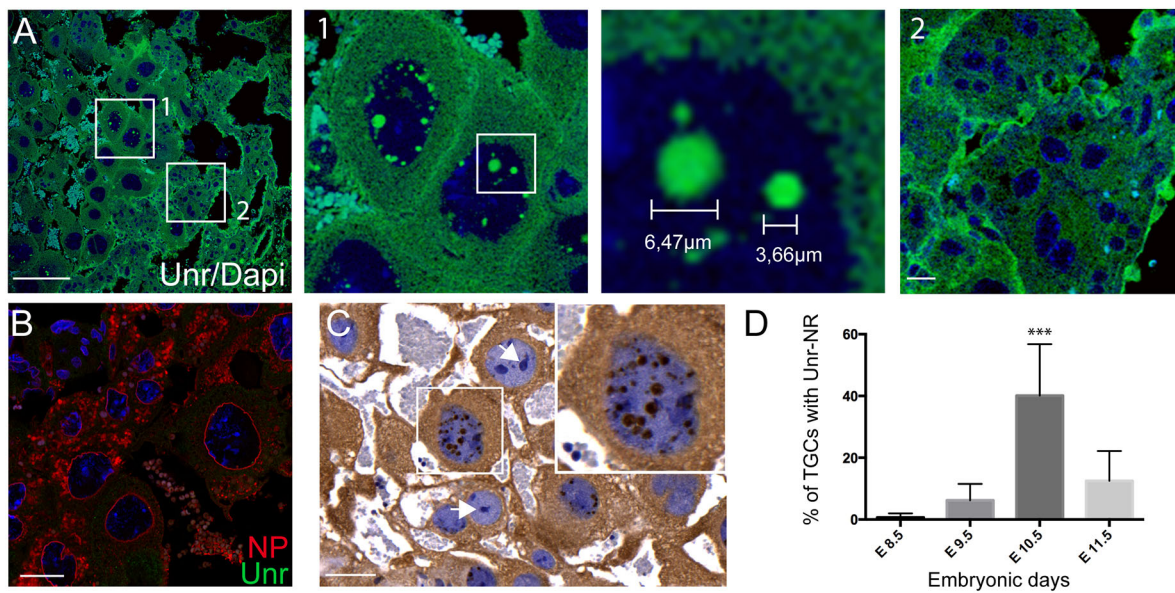


**Fig. 2. Unr localizes to discrete foci in nuclei of trophoblast giant cells.** (A) Unr immunofluorescence staining of representative sections from wild-type placentas at E10.5. DAPI was used to visualize nuclei. (A) Unr staining (green) is detected in the cytoplasm of spongiotrophoblasts (1) and trophoblast giant cells (2) of wild-type placenta. Second and third panels show enlarged views ( $\times 5$  and  $\times 25$ , respectively) of boxed areas in first and second panel, respectively, that allowed measurements of the Unr foci size of TGCs. Fourth panel shows enlarged view ( $\times 5$ ) of boxed area in first panel of Sps. Scale bar: 150  $\mu\text{m}$ . (B) Confocal image of TGCs of *Unr* KO mice co-stained with antibodies against Unr (green) and the nuclear pore (NP, red). Scale bar: 100  $\mu\text{m}$ . (C) Immunohistochemical staining for Unr (brown) of a wild-type placental section, showing localization of Unr to nuclear foci in TGCs. Top right inset is an enlarged view ( $\times 5$ ) of the boxed region. Scale bar: 50  $\mu\text{m}$ . The counterstain is haematoxylin. (D) Histogram representing the quantification of TGCs positive for nuclear Unr foci between E8.5 and E11.5. Data are the mean percentage of Unr-foci-positive cells per field  $\pm$  s.d. (taken at  $\times 20$  magnification), four placentas analyzed at each stage.

(Fig. 2C,D) show that Unr foci were undetectable in TGCs at E8.5. The proportion of Unr-foci-containing TGCs increased up to 45% at E10.5, thereafter declining again. This temporal analysis revealed that Unr foci are transient structures that are regulated during placental development.

We next wanted to know whether Unr foci represent a novel type of intra-nuclear structure or whether they correlate with known intra-nuclear domains. In view of the RNA-binding properties of Unr, we focused on nuclear structures known to be involved in RNA metabolism. We first observed, by immunohistochemistry staining, that Unr foci are large (average diameter  $4.03 \mu\text{M} \pm 1.07$ ,  $n=100$ , Fig. 2A) and clearly distinct from nucleoli (shown in Fig. 2C).

We then thought to determine whether the Unr foci are sub-nuclear bodies without membranes, or whether they are nuclear bodies wrapped by the nuclear envelope (Mao et al., 2011). Co-labeling of TGCs with antibodies against Unr and lamin A/C, and with DAPI (Fig. 3A) revealed that Unr foci are enclosed by the nuclear lamina and devoid of DNA (absence of DAPI staining, Fig. 3A, right panel). Of note, Unr was highly concentrated within these foci as revealed by the comparative quantification of the Unr protein in nucleoplasm, cytoplasm and Unr foci (Fig. S2A). Because Unr foci are surrounded by nuclear lamina and devoid of DNA, they might correspond to either the NR or to the infoldings of the inner nuclear membrane (INM). The NR consists of double nuclear membranes with embedded nuclear pores that are continuous with the endoplasmic reticulum (ER) and enclose a cytoplasmic core (Fricker et al., 1997; Malhas et al., 2011). INM infoldings are invaginations of the INM alone. They lack nuclear pore complex components and do not contain a cytoplasmic core (Jokhi et al., 2013; Speese et al., 2012). By using a combination of confocal immunofluorescence and transmission electronic microscopy (TEM) for the imaging of TGC sections, we

determined that Unr foci: (i) are lined by a double wall nuclear membrane containing nuclear pores – marked by antibodies against the nuclear pore complex (NP) and visible in TEM images (Fig. 3B), (ii) contain ER – marked by antibodies against the ER resident protein calnexin and visible in TEM images (Fig. 3C) and, (iii) are continuous with the cytoplasm (Fig. 3D). These results indicate that Unr foci are structurally similar to the NR. In agreement, we found that Unr foci contain cytoskeletal cytoplasmic elements (vimentin and  $\alpha$ -tubulin, Fig. S2B) that are frequently found in NRs (Gehrig et al., 2008). We next investigated whether Unr foci, as the NR, form a network of invaginations that is connected to the nuclear envelope. We performed 3D reconstruction by using confocal serial sections through the nucleus of a TGC co-stained with antibodies against Unr and Lamin A/C. Visualizing Unr foci from  $xy$  and  $z$  vantage points revealed that the observed dots ( $xy$  plane) are cross sections of tubular extensions of the nuclear membrane, clearly observed in the  $xz$  and  $z$  images (Fig. 3D and Movie 1). All Unr foci that we visualized in 3D appeared to form a network of branched tubular and vesicular structures in continuity with the nuclear membrane.

These results show that Unr is not expressed in nuclear bodies, and we identified a pronounced structural similarity between Unr foci and the NR, a network of cytoplasmic invaginations in the nucleus. Accordingly, we named this structure the Unr-rich NR (Unr-NR), i.e. the nuclear foci that contain Unr.

#### Unr-NRs concentrate poly(A) RNA, translation factors and ribosomes

The high concentration of Unr throughout the tubular network suggested a function of Unr-NRs in mRNA metabolism that had never been described for the NR. To determine whether Unr-NRs contained poly(A) RNA, we combined RNA *in situ* hybridization –

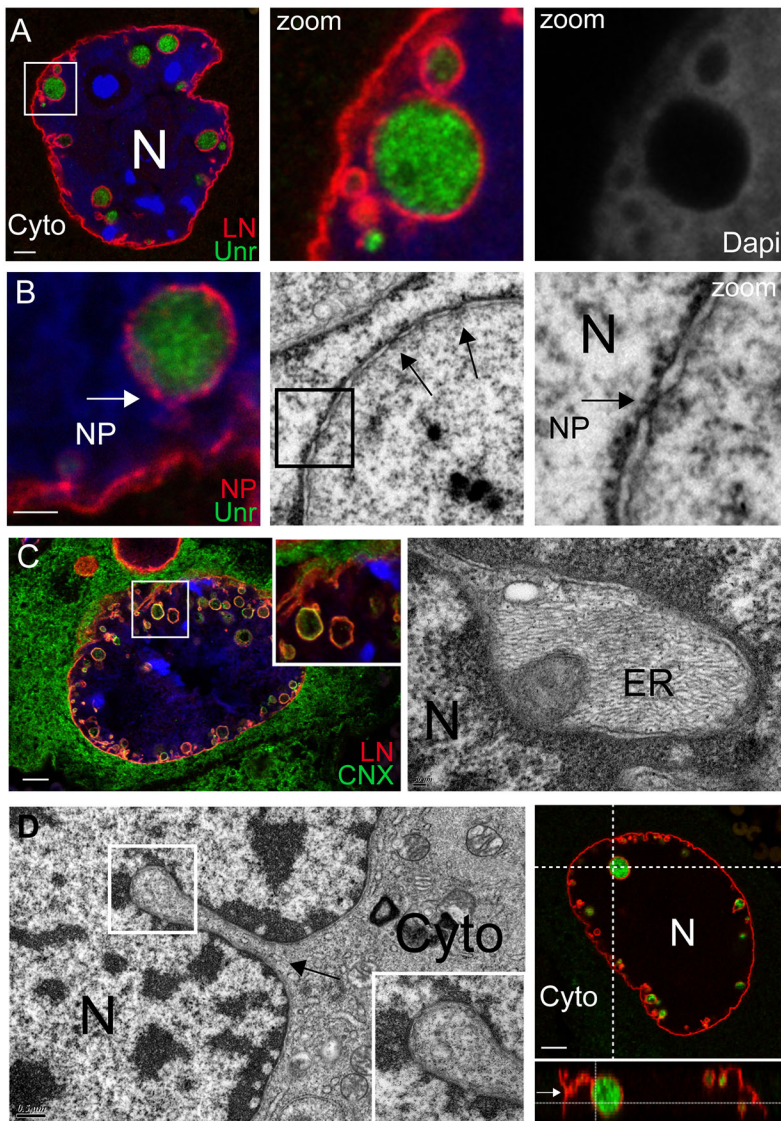


**Fig. 3. Immunostaining and TEM analyses showing that Unr foci are related to the NR structure.** (A) Unr foci are surrounded by nuclear lamina and devoid of DNA. TGCs were double-stained with antibodies against Unr (green) and Lamin A/C (LN, red). Scale bar: 5  $\mu$ m. Middle panel, magnification ( $\times 5$ ) of the boxed region. Right panel, DAPI staining of the boxed region. (B) Unr foci are wrapped by nuclear envelope studded with nuclear pores. Left panel, confocal image of TGCs double-stained with antibodies against Unr (green) and the nuclear pore complex (NP, red); scale bar: 10  $\mu$ m. Middle panel, TEM micrograph showing a nuclear pore (arrows). Right panel, magnification ( $\times 4$ ) of the boxed region (arrow indicates nuclear pores). (C) Unr foci contain ER. Left panel, Confocal image of TGCs double-stained with antibodies against lamin A/C (LN, red) and the ER protein calnexin (CNX, green). Top right inset is magnification ( $\times 2$ ) of the boxed region. Scale bar: 10  $\mu$ m. Right panel, TEM micrograph, showing ER sheets in nuclear invagination. (D) Unr foci have a tubular structure, continuous with the cytoplasm. Left panel, TEM micrograph showing an invagination of the nuclear envelope enclosing a cytoplasmic core (Cyto) indicated by an arrow. Inset shows magnified image ( $\times 1.75$ ) of the boxed region. Scale bar: 0.5  $\mu$ m. Right panel, 3D analysis of a representative TGC with Unr granules co-stained with anti-Unr and anti-lamin A/C antibodies. A unique 0.3  $\mu$ m confocal section shows the xy plane; serial confocal sections (1  $\mu$ m each) spanning the nucleus were used to reconstruct the yz plane (right side) and xz planes (bottom). The white dashed lines represent the cutting position for the analysis. Note the continuity between the Unr granule and the nuclear membrane (white arrow). Scale bar: 5  $\mu$ m.

by using a fluorescent FITC-labeled oligonucleotide (dT) probe – and immunofluorescence, by using antibodies against lamin A/C to outline the Unr-NR. An intense oligo (dT) signal was detected in 100% of the Unr-NRs examined, and the signal was sensitive to RNase treatment (Fig. 4A). To better characterize the spatial organization of the RNA within Unr foci, we performed triple-staining analyses combining RNA FISH and immunofluorescence, by using antibodies marking the NPC and the ER (Fig. S2C). The fluorescent signals corresponding to the poly(A) RNA (green) and the ER (red) did not colocalize within the Unr-NR but were closely apposed, revealing an intermingled organization of these components within the Unr-NR.

This spatial organization, i.e. poly(A) RNA concentrated in the vicinity of nuclear pores and the ER, suggests that Unr-NRs are sites of active translation of newly exported mRNAs. As mRNAs exit the nucleus, they undergo a pioneer round of translation, initiated by the cap-binding complex (CBC) comprising NCBP1 and NCBP2 (Maquat et al., 2010). The CBC is then replaced by the main translation initiation factor 4E (eIF4E), which directs steady-state rounds of mRNA translation. Poly(A)-binding protein nuclear 1 (PABPN1) is then replaced by poly(A)-binding protein cytoplasmic 1 (PABPC1) at the poly(A) tail (Hosoda et al., 2006; Lemay et al.,

2010). In TGCs, we examined the sub-cellular localization of NCBP2, eIF4E, PABPN1, PABPC1 and of the elongation factor eEF2 through coimmunostaining experiments by using Lamin A/C antibodies to delineate Unr-NRs. The specificity of these colocalization experiments was demonstrated in Unr-NRs by the absence of survival of motor neuron 1 and 2 (SMN1 and 2, respectively) RNA-binding proteins, not linked to mRNA translation (Fig. 4G). We found that all these factors, except NCBP2, localized and were concentrated within Unr-NRs (Fig. 4B–F). Because NCBP2 is replaced by eIF4E, the pioneer round of translation was likely to be completed for most of the transcripts. However, the presence of both PABPN1 and PABPC1 is surprising, and might be related to the reported cytosolic function of PABPN1 (Lemay et al., 2010).

Next, we used TEM to determine whether the ER present in Unr-NRs is studded with ribosomes. High-magnification TEM micrographs showed that free ribosomes as well as ER-bound ribosomes are clearly visible within these nuclear bodies (Fig. 4H).

Together, these results, showing that poly(A) RNA, translation factor as well as ribosomes are concentrated within Unr-NRs, support a role of these structures in mRNA translation. Since a role of NRs in mRNA metabolism has never been reported, our next

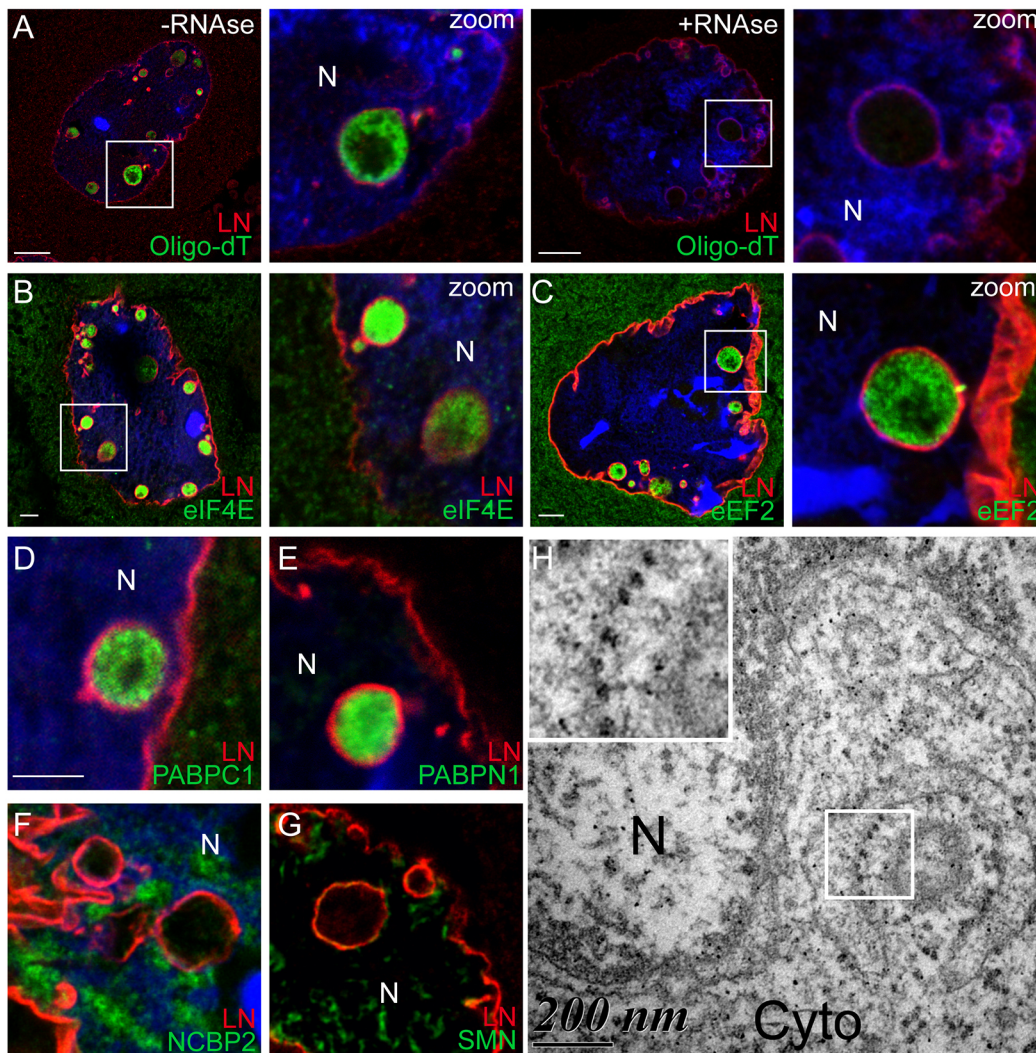


**Fig. 4. Unr-NRs concentrate poly(A) RNA, translation factors and ribosomes.** (A) Immunostaining for lamin A/C (red) was combined with FISH using an FITC-oligo(dT) probe (green) to locate poly(A) RNA in TGC nuclei (N). First and second panels: no RNase treatment. Third and fourth panels: the section was treated with RNase A before hybridization with the oligo(dT) probe. Two adjacent sections were analysed and images were acquired using the same exposure time. Second and fourth panels, respectively, are magnifications ( $\times 3.8$ ) of boxed regions in first and third panels, showing a strong oligo (dT) signal in Unr-NR (no RNase), with a heterogeneous sub-localization within the NR. Scale bars: 10  $\mu\text{m}$ . (B–G) Translational factors localize to Unr-NRs. TGCs were double-stained with antibodies against Lamin A/C (LN, red) and, in B: eIF4E (green), in C: eEF2 (green), in D: PABPC1 (green), in E: PABPN1 (green), in F: NCBP2 (green), in G: SMN (green). Images to the right of panels B and C are magnifications ( $\times 3.8$ ) of the respective boxed regions. Scale bars: 5  $\mu\text{m}$  (B–D). (H) TEM micrograph of a TGC showing free ribosomes or as arranged as ‘rosettes’ (polysomes, boxed region) located in a nuclear invagination. Inset is a magnification ( $\times 2.3$ ) of the boxed region. Scale bar: 200 nm.

efforts were aimed at determining (i) whether Unr-NRs are present in other tissues and cell lines and (ii) whether Unr-NRs are sites of active mRNA translation.

#### ***In vivo*, Unr-NRs are specifically found in polyploid cells**

We next used Unr immunohistochemistry to analyse Unr expression in a murine tissue microarray with 27 cores and in paraffin-embedded embryos (examples are shown in Fig. S1C–F). This screening revealed that none of the examined tissues contained Unr-NRs except liver, which we further studied by using immunofluorescence. The Unr-NRs present in hepatocytes were highly similar to those of TGCs, i.e. consisting of nuclear membrane invaginations in which Unr, poly(A) RNA and translation factors were concentrated (Fig. 5A,B). A tubular structure reaching deep in the nucleus was also visualized, (Fig. 5C and Movie 2); however, with a less-branched organization as that seen in TGCs. As a result,

the number of Unr-NRs per nucleus appeared to be lower in hepatocytes than in TGCs. That Unr-NRs are restricted to liver – in addition to the placenta – sustains the idea that Unr-NR formation is linked to polyploidy. In agreement, quantitative analysis of nuclear areas and DAPI intensities (Fig. 5D) showed that hepatocyte nuclei containing Unr-NRs were approximately two-fold larger and had an approximately two-fold higher DNA content than hepatocytes devoid of Unr-NRs.

#### ***In vitro*, Unr-NRs are related to both stress and polyploidy**

NRs have been described *in vitro* in a variety of cultured cells (Malhas et al., 2011) but their Unr content has not been investigated. It is, therefore, conceivable that Unr-NRs and NRs are identical structures, and NRs might have a not-yet-explored role in mRNA metabolism. To address this question, we used confocal microscopy to examine MDA-MB-231 cells, reported to present the highest

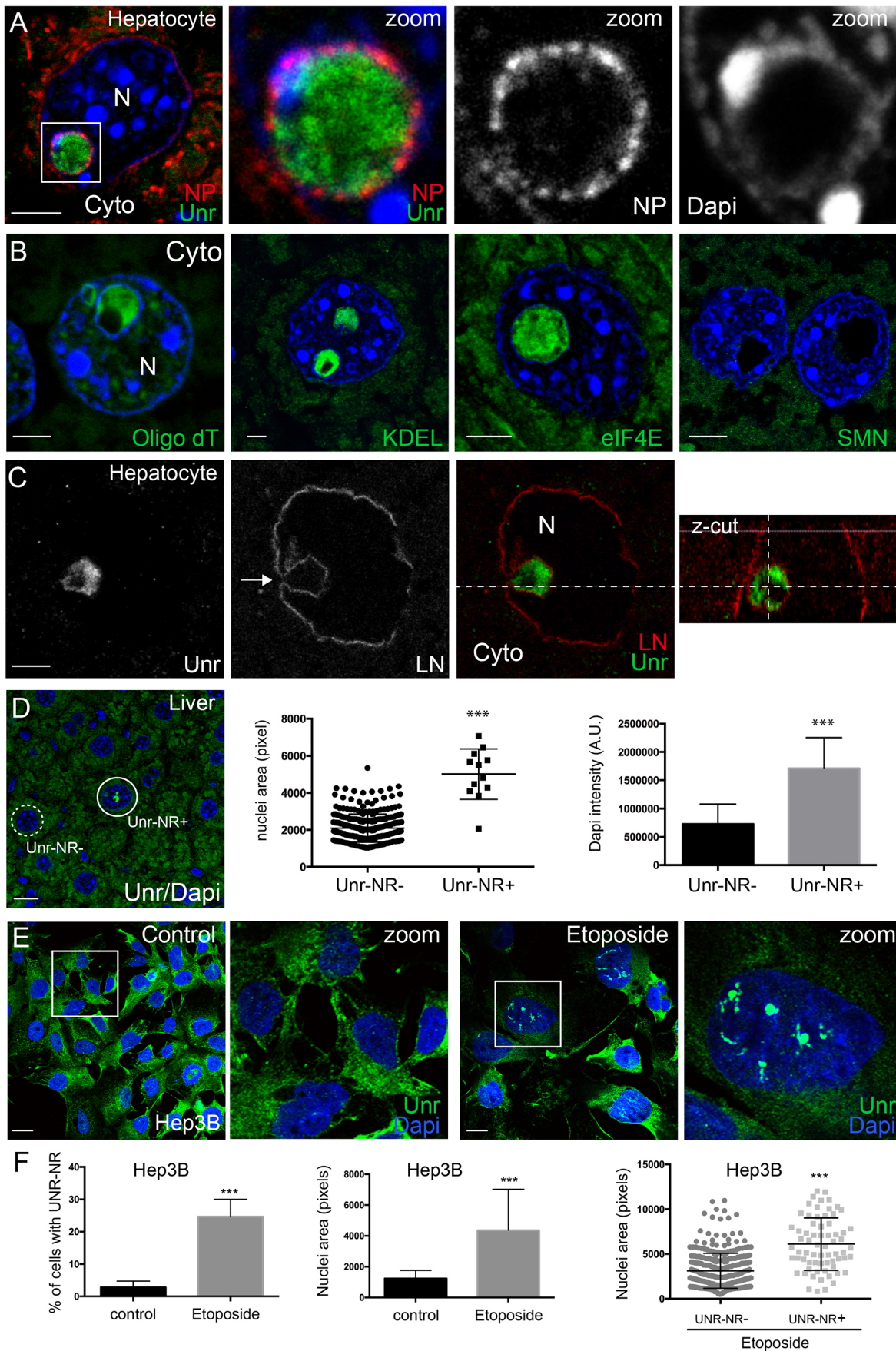


Fig. 5. See next page for legend.

**Fig. 5. Unr-NRs are found in mouse hepatocytes.** (A) Immunostaining analyses of representative sections from adult mouse liver. DAPI (blue) was used to visualize nuclei. Sections were double-stained with antibodies against Unr (green) and the nuclear pore (NP, red). The third and fourth panels, respectively, show NP and DAPI fluorescence in gray. Second panel: Magnification ( $\times 3.8$ ) of boxed area in the first panel. Scale bar: 5  $\mu\text{m}$ . (B) First panel: poly(A) RNA detection by FISH (green); second, third and fourth panels: Confocal images of liver sections stained with antibodies against the KDEL peptide marking ER proteins or the translation factor eIF4E (second and third panels, green) and the SMN protein as negative control (fourth panel, green). DAPI (blue) was used to visualize nuclei. Scale bars: 5  $\mu\text{m}$ . (C) Immunostaining analyses showing that Unr-NRs visualized in hepatocytes form a tubular structure continuous with the nuclear membrane. First, second and third panels: Immunofluorescence analysis of a liver section co-stained for Unr (green) and lamin A/C (LN, red), with first and second panels showing staining in gray. Overlay of the signals (constituting the 1  $\mu\text{m}$  confocal section shown in the the xy plane) is shown in the third panel. Fourth panel: 3D analysis; serial confocal sections (1  $\mu\text{m}$  each) spanning the nucleus were used to reconstruct the yz plane (right) and xz planes (bottom). Scale bar: 5  $\mu\text{m}$ . (D) Quantification of hepatocytes exhibiting Unr-NRs. First panel: Representative field of a liver section immunostained with anti-Unr antibodies (green) and counterstained with DAPI (blue) is shown. Second panel: Distribution of the nuclear area of hepatocytes without (Unr-NR $^-$ ,  $n=60$ ) or with (Unr-NR $^+$ ,  $n=12$ ) Unr-NRs. Third panel: Quantification of DNA content in nuclei of hepatocytes that lack (Unr-NR $^-$ ) or contain (Unr-NR $^+$ ) Unr-NRs. DNA content was quantified through the intensity of DAPI-integrated fluorescence. Data are the average of  $\sim 100$  nuclei per field  $\times 30$  fields  $\pm$  s.d. \*\*\* $P < 0.0001$ . (E,F) Unr-NRs are formed in Hep3B cells when treated with etoposide. (E) Confocal images of Hep3B cells co-stained with antibodies against Unr (green) and lamin A/C (red). DAPI (blue) was used to visualize nuclei. Representative fields of normal (first panel) and etoposide-treated (third panel). Second, and fourth panels, respectively, are magnifications ( $\times 5$ ) of the boxed areas in first and third panels. Scale bars: 10  $\mu\text{m}$ . (F) Quantifications of Hep3B cells exhibiting Unr-NRs. Left panel: Quantification of Hep3B cells positive for Unr-NRs in control or etoposide-treated cells. Middle panel: Quantification of nuclear areas in control or etoposide-treated cells. Right panel: Distribution of the nuclear area of etoposide-treated cells without (Unr-NR $^-$ ,  $n=60$ ) or with (Unr-NR $^+$ ,  $n=12$ ) Unr-NRs.

ratio of NRs per cell (Johnson et al., 2003). Although we detected double-wall nuclear membrane invaginations devoid of DNA (Fig. S3A), and containing microtubules (Fig. S3B), these structures neither concentrate Unr nor eIF4E (Fig. S3A, C). Based on their expression profile, Unr-NRs, therefore, do not correspond to the classic NRs.

Since *in vivo* the presence of Unr-NRs was restricted to polyploid cell types, we reasoned that, *in vitro* also, hyperploidy might be essential for Unr-NRs formation. To this end, we selected two human cancer cell lines, BeWo and Hep3B – derived from trophoblasts and hepatocytes, respectively – to test the capacity of cytotoxic treatments known to induce polyploidy to trigger Unr-NRs formation. The drugs we used included etoposide – a DNA-damaging drug, and Taxol – a spindle toxin (Litwiniec et al., 2013; Marth et al., 1995). Whereas Unr-NRs were detectable in untreated cultures, their incidence markedly increased following drug treatment in both cell cultures (Figs 5E and 6A). The proportion of Unr-NR-containing cells reached  $\sim 23\%$  in etoposide-treated Hep3B cells and  $\sim 70\%$  in Taxol-treated BeWo cells (Figs 5F and 6B, left panels). Quantitative analysis of nuclear areas revealed that, simultaneously, etoposide and Taxol induced a  $\geq$ two-fold enlargement of nuclei (Figs 5F and 6B, middle panels). Moreover, in this cell population, nuclei of Unr-NR-positive cells were twice as big (Figs 5F and 6B, right panels).

We then extended our investigations to two further cancerous human cells lines of other origin, MDA-MB231 and HCT116, derived from breast and colon cancer, respectively. We found that Unr-NRs, barely detectable in untreated cell cultures, were efficiently induced by etoposide in MDA-MB231 cells

(Fig. S3D,E). As in BeWo and Hep3B cells, Unr-NRs appeared in MDA-MB231 cells with enlarged nuclei (Fig. S3E). Fig. S3F presents a clear Unr-rich nuclear invagination, observed in MDA-MB231 cells. We did not detect Unr-NRs in HCT116 cells, whatever the dose of etoposide or Taxol used.

In summary, we infer from these results that, *in vitro*, Unr-NR formation is related to both stress and polyploidy. Moreover, cancer cells treated with anticancer drugs seem prone to form Unr-NRs (three Unr-NR-positive cell lines of four cell lines tested).

### Unr-NRs are sites of active translation

The development of *in vitro* cell culture models made it possible to decipher the translational status of mRNAs localized to Unr-NRs. Since Taxol treatment of BeWo cells turned out to be the most effective in UNR-NRs induction, we selected this condition for further analyses. First, we confirmed that the *in vitro* formed Unr-NRs were highly similar to their *in vivo* counterpart. Indeed, in Taxol-treated BeWo cells, Unr, eIF4E, and poly(A) RNA were concentrated in nuclear membrane invaginations (Fig. 6A,C).

To directly visualize localized translation in live cells, we used the ribopuromylation method (RPM), which works on the basis that puromycin (PMY) is incorporated into nascent chains, whose association with ribosomes is maintained by the presence of the chain elongation inhibitor emetine (David et al., 2012). In control BeWo cells, RPM coupled with PMY staining produced an intense signal, distributed throughout the cytoplasm, and co-localized with Unr (Fig. 6D,E, left panels). Blocking translation by anisomycin before the puromycin pulse abrogated the PMY signal (Fig. 6D, right panels), demonstrating the specific labeling of ribosome-associated nascent chains by the PMY antibodies. In Taxol-treated BeWo cells, the distribution of the Unr and PMY signals clearly changed, Unr being mostly localized to Unr-NRs, whereas the PMY signal was observed both in the cytoplasm and in Unr-NRs (Fig. 6E; Fig. S4B,C). PMY and the ER marker calnexin showed a similar distribution, present in the cytoplasm of control cells, and in both the cytoplasm and Unr-NRs of Taxol-treated cells (Fig. S5C).

These results demonstrated that an active mRNA translation process is taking place within Unr-NRs ( $>80\%$  of the Unr-NRs were PMY positive). However, we cannot exclude that Unr-NRs also represent a storehouse for non-translating mRNAs. Indeed, a number of studies has provided evidence that cytoplasmic RNA granules are structures in which mRNAs are ‘masked’, i.e. in a translational repressed state (Anderson and Kedersha, 2009; Eulalio et al., 2007). To test whether Unr-NRs harbor non-translating mRNAs, we used antibodies against TIA-1 and Rck/p54 (also known as DDX6), markers shared by P granules, P-bodies and stress granules (Buchan and Parker, 2009). We observed that, in TGCs, most of the Unr-NRs appeared positive for TIA-1 and Rck/p54 (Fig. S2D), suggesting that Unr-NRs store a pool of non-translating mRNAs. But does active and repressed mRNA translation take place within Unr-NRs? To investigate this hypothesis, we performed RPM in live BeWo cells, coupled with PMY, Unr and TIA-1 triple staining. As expected, TIA-1 was undetectable in unstressed control cells (Fig. S4A). In Taxol-treated cells, TIA-1 was expressed in most Unr-NRs, and the PMY and TIA-1 signals colocalized within Unr-NRs (Fig. S4B).

Altogether, the aforementioned data suggest a dual role of Unr-NRs. On one side, they are sites of active mRNA translation and, on the other side, they are likely to maintain a pool of mRNAs in a translationally repressed state.

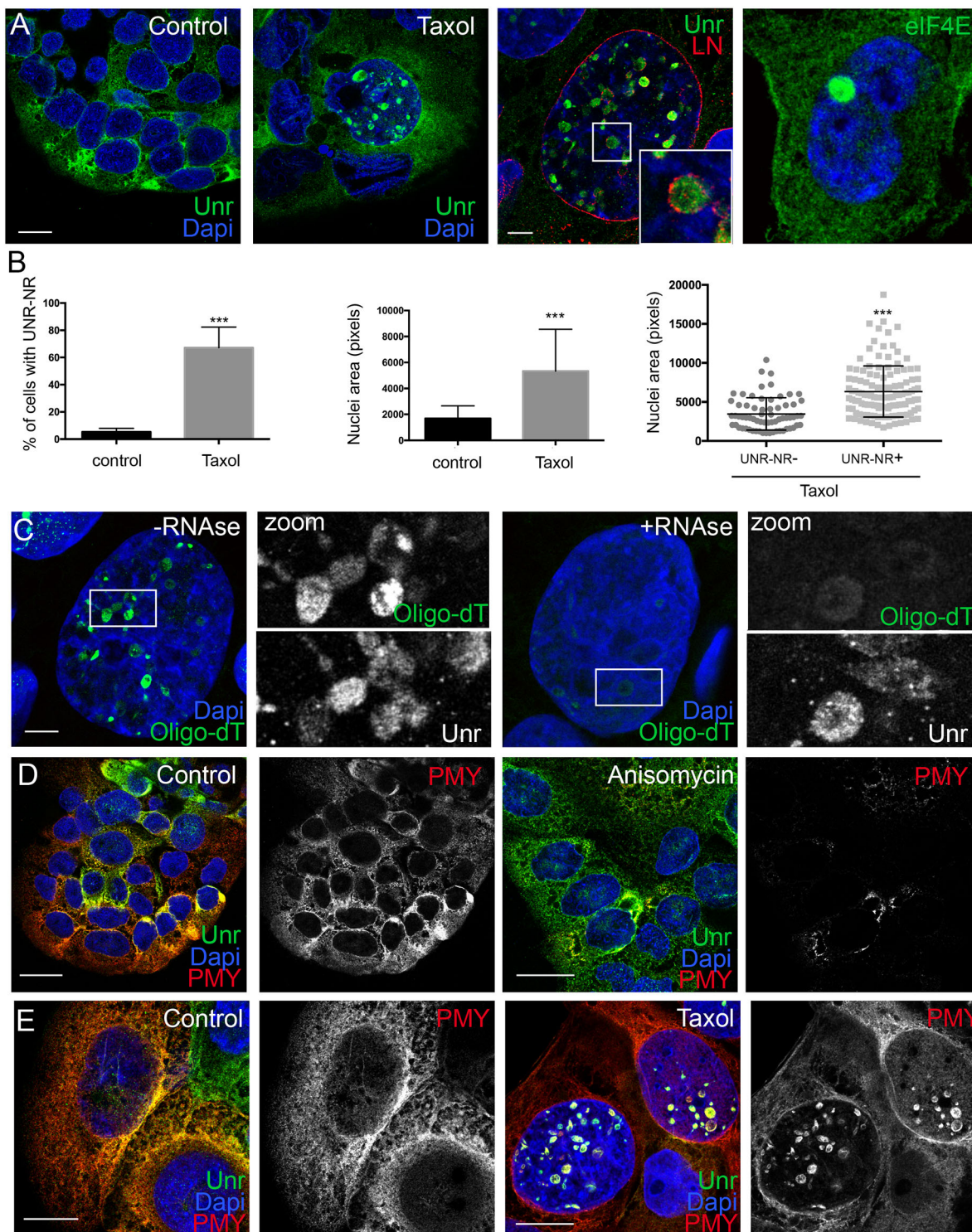


**Fig. 6. Unr-NRs are formed in BeWo cells treated with Taxol and represent sites of active mRNA translation.** (A) BeWo cells cultured without (first panel) or with  $0.5 \mu\text{M}$  Taxol for 48 h (second, third and fourth panels) and stained for Unr or eIF4E (fourth panel, green), LN (third panel, red); nuclei were counterstained with DAPI (blue) to evaluate their average size. Inset is third panel is the magnification of boxed area, showing a nucleus with Unr-NRs, co-stained for Unr (green) and Lamin A/C (red). DAPI was used to visualize nuclei and evaluate the average nuclear size. Scale bar:  $5 \mu\text{m}$ . (B) Quantification of BeWo cells exhibiting Unr-NRs. Quantification was carried out as described in Fig. 5F but cells had been treated with Taxol instead. (C) *In-vitro*-formed Unr-NRs contain poly(A) RNA. Double-staining of Taxol-treated BeWo cells for poly(A) RNA (green) and Unr (white) without (first and second panels) or with (third and fourth panels) RNase treatment. Scale bar:  $5 \mu\text{m}$ . (D, E) Nascent polypeptide chains are present within Unr-NRs. BeWo cells were pre-treated or not with  $40 \text{ nM}$  anisomycin for 30 min anisomycin (D: first or third panel, respectively), and with  $0.5 \mu\text{M}$  Taxol for 48 h or not (E: first or third panel, respectively). Cells were then double-stained for puromycin (anti-PMY, red) to label translating ribosomes and for Unr (anti-Unr, green) to label Unr-NRs. DAPI (blue) was used to visualize nuclei. Both fourth panels show PMY labeling in gray. Scale bars:  $5 \mu\text{m}$ .



### Unr is required for Unr-NRs formation

To address the role of Unr in the formation of Unr-NRs, we examined whether Unr-NRs are formed in TGCs null for Unr. To be able to visualize a nuclear tubular network in the absence of Unr, we used antibodies against the nuclear pore. Five placentas each of wild-type and *Unr* KO mice at E10.5 and three each at E11.5 were analyzed. By using either 2D or 3D confocal imaging, we found that the perinuclear membrane was stained normally in *Unr* KO TGCs, whereas intranuclear invaginations – that are visible as granules in cross sections – were completely absent (Fig. 7B). Moreover, the nuclei of *Unr*<sup>-/-</sup> TGCs neither accumulate ER resident proteins nor translation factors in NR-like structures in (Fig. 7C). *Unr*<sup>+/-</sup> TGCs did not differ from *Unr*<sup>+/+</sup> TGCs, regarding the proportion of Unr-NR-positive cells or their molecular composition. These results demonstrate that Unr is required for the formation of NR-like structures that concentrate polyadenylated RNA and translation factors in TGCs.

### DISCUSSION

In this study, we used an *Unr* knockout model to determine the role of this RNA-binding protein during mouse development. The two main findings are that Unr (a) is required for mouse embryonic and placental development, and (b) defines a novel type of NR by having a role in mRNA translation.

### Unr is required for placental and embryonic development in mice

*Unr* KO embryos die between E10.5 and E12.5 but the phenotypic defects they exhibit before death, i.e. absence of neural tube closure, delay in heart maturation and small size, are unlikely to be its cause (Copp, 1995). In contrast, major placental defects were evident.

These are presumably the primary cause for growth retardation and death of *Unr* KO embryos, as a result of insufficient materno-fetal nutrient exchanges. Thus, Unr – as several other RNA-binding proteins (Katsanou et al., 2009; Lu et al., 2005; Shibayama et al., 2009; Stumpo et al., 2004) – has important roles during mouse development.

### Unr defines a novel class of NR that is involved in mRNA translation

Unr expression studies revealed that, surprisingly, Unr is localized to bright foci within nuclei of a subset of TGCs. We determined that Unr foci were not isolated in the nucleus but were cross sections of a tubular network of nuclear membrane invaginations enclosing a cytoplasmic core. These structures are related to the NR (Fricker et al., 1997; Malhas et al., 2011) and, accordingly, were named Unr-NRs.

What is the role of Unr-NR? Several studies have provided evidence that NRs are involved in Ca<sup>2+</sup> signaling within localized sub-nuclear regions (Echevarria et al., 2003; Lui et al., 1998). Because of the Unr RNA-binding properties, we thought that Unr-NRs might have a role in mRNA metabolism that had not yet been explored in NRs (Malhas et al., 2011). And, indeed, we found that Unr-NRs present in TGCs are structures that contain an impressive amount of poly(A) RNA and translation factors. We then considered two possibilities: that (i) either a function in mRNA metabolism had not yet been explored in classic NRs, and Unr-NRs are not functionally different from classic NRs or (ii) they are two types of NR. The first, described in many cell types, does not concentrate the translational machinery and has been shown to be involved in Ca<sup>2+</sup> signaling; the second, Unr-NR, is restricted to specific cell types and has a function in mRNA metabolism. To

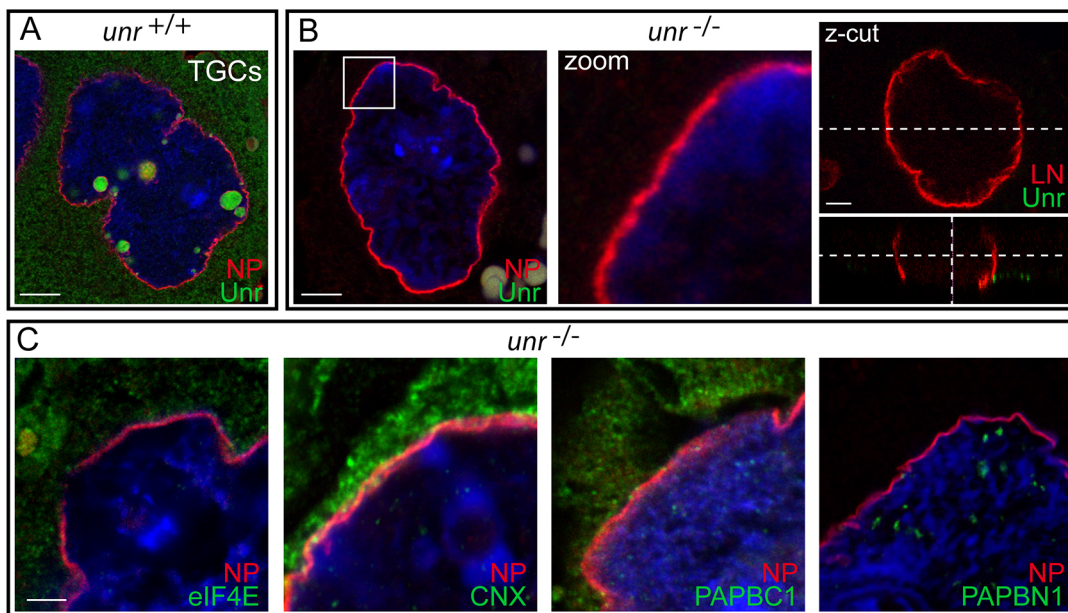


**Fig. 7. Unr is required for Unr-NRs formation.** Unr-NRs are not formed in *Unr* KO TGCs. Confocal images of TGCs co-stained with antibodies against Unr (green) and the nuclear pore (NP, red) are shown. (A) Wild-type TGC (positive control) with Unr-NRs. Scale bar: 10  $\mu$ m. (B) Absence of nuclear envelope invaginations in *Unr*<sup>-/-</sup> TGCs. (Left panel) Representative TGC magnification ( $\times 5$ ) of boxed area around the nuclear membrane (middle panel) showing enlarged view of a TGC. (Right panel) 3D analysis of a representative TGC from the placenta of a *Unr* KO mouse, co-stained with anti-Unr and anti-lamin A/C antibodies. A unique 0,3  $\mu$ m confocal section shows the xy plane; serial confocal sections (1  $\mu$ m each) spanning the nucleus were used to reconstruct the yz plane (right side) and xz planes (bottom). White dashed lines represent the cutting position for the analysis. Scale bars: 50  $\mu$ m (left panel), 5  $\mu$ m (right panel). (C) Absence of ER-resident proteins and translation factors in nuclei from *Unr*<sup>-/-</sup> TGCs. Confocal images of *Unr*<sup>-/-</sup> TGCs co-stained with antibodies against the nuclear pore (NP, red) and eIF4E, calnexin (CNX), PABPC1 and PABPN1 (green). DAPI was used to visualize nuclei. Scale bars: 5  $\mu$ m.

answer this question, we searched for Unr-NRs in a variety of cell types and generated *in vitro* cell culture models to analyse the function(s) of Unr-NR.

### Unr-NRs are related to both stress and polyploidy

In an effort to link Unr-NRs to cell physiology, we searched for these structures in murine tissues. A tissue microarray screen combined with immunohistochemistry analyses of some murine tissues revealed their scarcity since none of the examined tissues contained Unr-NRs, except liver, a tissue rich in polyploid cells (Chen et al., 2012; Pandit et al., 2012). The low incidence (3%) of Unr-NRs suggests that, in liver, the increased ploidy, modest as compared to that reached in TGCs (up to 1024 copies), is necessary but not sufficient to produce Unr-NRs. An adverse context, such as oxidative stress, might also contribute to their formation. It will be important to scrutinize other polyploid cell types not examined here, such as megakaryocytes and cardiomyocytes, to confirm the restriction of Unr-NRs to enlarged polyploid cells.

These findings helped us to generate cell culture models exhibiting Unr-NRs. Our hypothesis, linking Unr-NRs to polyploidy, was correct since Unr-NRs were inducible in the hepatoblastic Hep3B cell line treated with etoposide, and in the trophoblastic BeWo cell line treated with Taxol (Litwiniec et al., 2013; Marth et al., 1995). Unr-NRs were preferentially formed in cells with enlarged nuclei, their frequency in the surviving cell population reaching up to 23% in etoposide-treated Hep3B cells and 70% in Taxol-treated BeWo cells. Unr-NRs are not restricted to cell lines derived from placenta and liver because they are also efficiently induced by etoposide in breast-cancer-derived MDA-MB231 cells. Neither etoposide nor Taxol led to Unr-NRs formation in the colorectal-carcinoma-derived HCT116 cells. An hypothesis is that HCT116 cannot endoreplicate their genome because they express wild-type p53 (Liu and Bodmer, 2006), which is assumed to prevent cells from undergoing endoreduplication and polyploidy (Di Leonardo et al., 1997). BeWo, Hep3B and MDA-MB231 cells either express an inactive p53 protein, carry p53 mutations or lack p53 (Hau et al., 2006; Lin et al., 2000; Negrini et al., 1994).

### Unr-NRs are involved in mRNA translation

By using RPM, we demonstrated that Unr-NRs are sites of active mRNA translation. Nevertheless, a number of studies has provided evidence that mRNAs, aggregated as microscopically visible RNA granules, are translationally repressed (Anderson and Kedersha, 2009; Eulalio et al., 2007). Specific examples include germ cells, perinuclear P granules, P-bodies and stress granules that all share protein components including TIA-1 (Kedersha and Anderson, 2007). TIA-1 has been found in most (but not all) Unr-NRs, suggesting that a pool of untranslated mRNAs is also localized herein. As proposed for P granules (Sheth et al., 2010), newly exported mRNAs could be transiently stored in Unr-NRs because their diffusion rate into the cytoplasm is low.

That Unr-NRs are sites of active mRNA translation and storage is a somewhat unusual situation since most of RNA granules are dedicated to the storage of non-translating mRNAs. Two recent reports, however, have documented RNA granules either translationally active or as having a dual translational status, i.e. in which translated and untranslated mRNAs are both present (Buchan, 2014; Weil et al., 2012; Yasuda et al., 2013).

### Benefits of Unr-NR formation

A diagram illustrating the structure and function of Unr-NRs is presented in Fig. 8. We propose that the formation of Unr-NRs is an

adaptive response of the cell following metabolic or cytotoxic stress situations. TGCs encounter a metabolic stress condition because of their vastly amplified genome producing an amount of mRNA that exceeds their capacity of translation. We propose that, in order to cope with this stress, polyploid TGCs expand the nucleocytoplasmic interface and the ER compartment by forming the Unr-NR network, which then facilitates mRNA export and translation at the rough ER. They also maintain a pool of untranslated mRNAs localized within the core of the Unr-NR network. This model is consistent with recent reports having established that, under stress conditions, mRNA translation on free ribosomes is repressed, whereas mRNA translation on ER-bound ribosomes is sustained (Lerner and Nicchitta, 2006; Unsworth et al., 2010).

Many questions arise from the results reported here. Unr-NRs are regulated structures, appearing at a precise developmental stage of the placental development or in response to cytotoxic stresses. A current theme is that polyploidy confers resistance to environmental stresses not tolerated by diploid cells (review in Schoenfelder and Fox, 2015). It will be very interesting to see whether Unr-NRs facilitate survival of giant cancer cells that are subjected to chemotherapy.

### Unr is required for the formation of Unr-NRs

Finally and importantly, we determined that Unr-NRs do not form in Unr-null TGCs in the absence of Unr. What is the role of Unr in Unr-NR formation? Although the role of Unr is a matter of speculation, we propose that Unr (a) promotes the nuclear and membrane expansion required for the acquisition of a NR, by stimulating lipid and protein synthesis (Gehrig et al., 2008); (b) recruits mRNAs fated to be translated on ER-bound ribosomes. This later possibility relies on Unr being located at the ER, a position that is conserved between *Drosophila* and mammals (Abaza et al., 2006; Jacquemin-Sablon et al., 1994).

### Conclusion

In conclusion, the main finding of this study is the identification of an Unr-rich structure that we have named Unr-NR because of its structural similarity with the NR. The novelty of this structure, identified *in vitro* and *in vivo*, is that it comprises a the high amount of poly(A) RNA and translation factors and that its function in mRNA translation that has not been reported previously. Unr-NRs – like NRs – are not found in normal cells, but are restricted to polyploid cells (*in vivo*) and to stressed cells (*in vitro*). We propose that this novel type of NR provides an extended surface for mRNA translation at the rough ER, helping cells to ensure correct translational control. Our results, linking Unr-NRs to cancerous cells subjected to anticancer drugs, might be of importance for drug resistance.

### MATERIALS AND METHODS

#### Unr-deficient mice and genotyping

Unr<sup>+/-</sup> mice were obtained as previously described (Boussadia et al., 1997). Unr<sup>+/-</sup> mice were maintained on a C57BL/6 genetic background. Mice were routinely genotyped by PCR of tail DNA. Embryos were genotyped by PCR of yolk sac DNA at E9.5, and by PCR at earlier stages. This study was performed in accordance with the European Community Standards on the Care and Use of the Animals and was approved by the Animal Care and Use Committee of the University of Bordeaux. Adult livers were obtained from C57-BL/6, Nog or NMRI mice.

#### Primers

Primers used for genotyping. The targeted allele was detected by using neo primers (neoFo 5'-CGTGTCCGGCTGTCAGCGCAGG-3'; neoRo 5'-CAACGCTATGTCCTGATAGCGGTCC-3') that give a product of

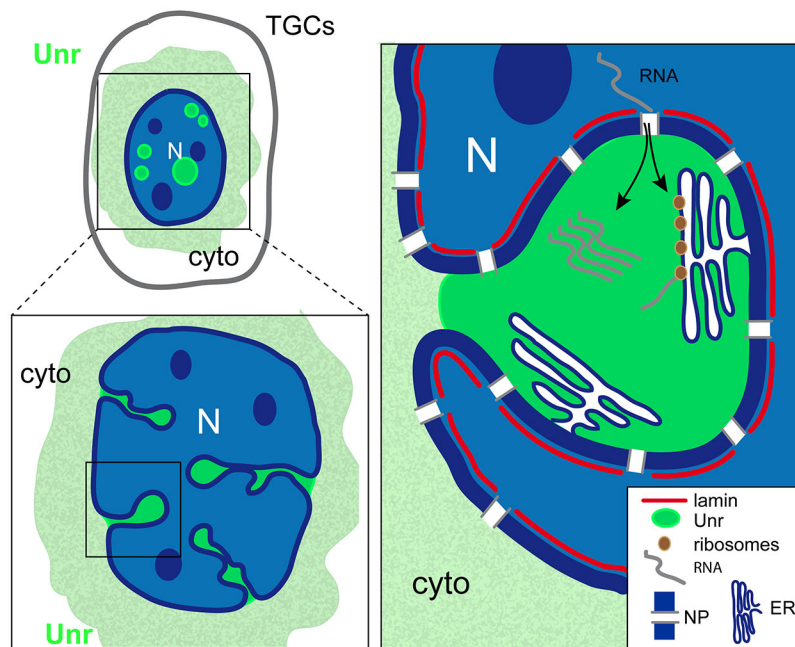


**Fig. 8. Schematic of a wild-type TGC exhibiting Unr-NRs.** Left: Whole-cell view (top) and view of the nucleus (enlarged, bottom). Right: Schematic of Unr-NR and its main components identified in this work.

565 bp. The normal allele was detected by using *Unr* promoter primers (unrFw 5' -AACGCAGAGATTGCTTCTGG-3'; unrBw 5'-CCACTTTA-ACAGTGAGGTCG-3') that give a product of 290 bp.

#### Cell culture and drug treatment

BeWo (human trophoblast-derived choriocarcinoma) cells were maintained in Ham's F-12 K medium (Gibco) supplemented with 2 mM L-glutamine, 20% fetal bovine serum and 100 U/ml penicillin–streptomycin (Invitrogen). Hep3B (human hepatocellular cell carcinoma), MDA-MB231 (human breast cancer) and HCT116 (human colorectal carcinoma) cells were maintained in DMEM containing 4.5 g/l glucose, supplemented with 10% fetal bovine serum and 100 U/ml penicillin–streptomycin. For Unr-NR induction, BeWo, Hep3B and MDA-MB231 cells were plated in 24-well dishes ( $4 \times 10^4$  cells/well); 24 h later, BeWo cells were treated with 0.5  $\mu$ M Taxol (paclitaxel; Sigma) or 0.2% DMSO (as vehicle) for 48 h. The medium with Taxol or 0.2% DMSO was changed every 24 h. Hep3B and MDA-MB231 cells were treated with 1.5  $\mu$ M etoposide for 24 h (Hep3B) or 48 h (MDA-MB231), and cultured for an additional 48 h in drug-free medium (Hep3B).

#### Histology and immunohistochemistry

Embryos, yolk sacs, placentas were fixed at 4°C in 4% paraformaldehyde in PBS for 2 h – adult livers were fixed overnight, rinsed in PBS, dehydrated in graded ethanol, cleared in toluene and embedded in paraffin. Sections (4  $\mu$ m) were stained with hematoxylin and eosin (H&E) following standard protocols, or used for immunohistochemistry. Antigens were retrieved by 30 min incubation at 98°C in target-retrieving solution (10 mM Tris-HCl pH 9, 1 mM EDTA) followed by 30 min cooling at room temperature. Sections were incubated for 2 h at room temperature with primary antibody (anti-Unr; 1:100, HPA018846, Sigma), and bound antibodies were visualized by using the anti-rabbit or anti-mouse RTU Vectastain Kit (Universal Elite ABC Kit, PK-7200, Vector) and NovaRED Substrate Kit (SK-4800, Vector). Nuclei were detected by light counterstaining with Mayer's hemalun.

#### Immunofluorescence

##### Tissue sections

After deparaffinization and antigen retrieval, sections were incubated in a blocking solution (1% BSA and 10% SVF in PBS) for 30 min and with primary antibodies for 1 h at room temperature. Sections were then incubated with Alexa Fluor-conjugated secondary antibodies for 1 h before mounting in DAPI Fluoromount-G (SouthernBiotech).

#### Cell cultures

Cells grown on coverslips were fixed with 4% paraformaldehyde in PBS for 10 min, permeabilized with 0.2% Triton X-100 for 10 min before incubation with antibodies as described above.

#### Antibodies

The following primary antibodies were used in this study: anti-Unr (1:100, HPA018846, Sigma), anti Lamin A/C (1:500, provided by Harald Wodrich, UMR-CNRS5234, Bordeaux, France), anti-nuclear pore complex (1:100, clone Mab414, ab24609, Abcam), anti-Calnexin (1:100, ab93355, Abcam), anti-KDEL (1:100, clone 10C3, Enzo Life Sciences), anti-vimentin (1:40, clone V9, Dako), anti-alpha tubulin (1: 100, clone DM1A, Sigma-Aldrich), anti-eIF4E (1:100, clone 87, BD Transduction Laboratories), anti-NCBP2 (1:100, ab124632, Abcam), anti-PABPN1 (1:100, AJ1580b, Abgent), anti-PABPC1 (1:100, clone 10E10, Sigma-Aldrich), anti-eEF2 (1:100, ab40812, Abcam), anti-SMN (1: 100, 610647, BD Transduction Laboratories), anti-PMY (1:100, Millipore, MAbE343), anti-TIA-1 and anti-Rck/p54 were gifts from Hervé Moine and Catherine Tomasetto (Université Louis Pasteur, Illkirch, France) (1:500 each). Secondary antibodies used were: Alexa Fluor 488-, Alexa Fluor 594- and Alexa Fluor 647-coupled anti-mouse and anti-rabbit, anti-goat and anti-guinea-pig (1:400, Life Technology). DNA was visualized with DAPI (0.5  $\mu$ g/ml).

#### RNA FISH

RNA fluorescence in situ hybridization (FISH) on paraffin-embedded tissue sections was performed according to de Planell-Saguer et al. (2010). After deparaffinization and antigen retrieval, sections were incubated with prehybridization solution (4 $\times$  SSC, 10% formamide) for 20 min at room temperature. Where prehybridization RNase treatment was applied, sections were treated with 0.1  $\mu$ g/ $\mu$ l RNase A in PBS for 2 h at room temperature. Hybridization was performed for 1 h at room temperature, in hybridization solution (4 $\times$ SSC, 10% formamide, 0.5 mg/ml single-stranded DNA, 0.5 mg/ml tRNA, 10% dextran) containing FITC-conjugated oligo (dT)<sub>40</sub> probe (Eurogenetec) at a final concentration of 0.5 ng/ $\mu$ l. After washes, sections were either mounted and examined, or subjected to immunofluorescence before mounting.

For RNA FISH on cell cultures, cells were fixed in 4% paraformaldehyde for 10 min at room temperature, washed in PBS and permeabilized for  $\geq 24$  h in 70% ethanol at 4°C. Prior to hybridization, coverslips were incubated in 2 $\times$ SSC, 15% formamide, at 65°C for 10 min. Hybridization and washes were carried out as described above, except that hybridization was performed for 16 h at 37°C.

## Ribopuromycylation

To visualize newly synthesized proteins within cells, we used the ribopuromycylation (RPM) method as described by David et al. (2012). BeWo cells grown on coverslips were incubated for 15 min at 37°C in complete H12 medium supplemented with 208 µM emetin (EMD, Sigma). In protein synthesis inhibitor control experiments, cells were pretreated with 40 µM anisomycin (Sigma) for 30 min at 37°C before incubation with EMD. Cells were then treated with 355 µM cycloheximide (Sigma) for 2 min on ice in permeabilization buffer [50 mM Tris-HCl pH 7.5, 5 mM MgCl<sub>2</sub>, 25 mM KCl, 0.015% digitonin, EDTA-free protease inhibitor, 10 U/ml RNaseOut (Invitrogen)]. Cells were then washed and incubated on ice in polysome buffer (50 mM Tris-HCl pH 7.5, 5 mM MgCl<sub>2</sub>, 25 mM KCl, 0.2 M sucrose, EDTA-free protease inhibitor, 10 U/ml RNaseOut) supplemented with 91 µM puromycin (PMY, Sigma) for 10 min. After rapid washing in polysome buffer, cells were fixed in 4% formaldehyde for 15 min at room temperature. After fixation, cells were washed twice with PBS and immunostained with anti-PMY antibody as described above.

## Image acquisition

### Histology and immunohistochemistry

Slides were scanned by using a digital slide scanner (Pannoramic Scan; 3D HISTECH Ltd, Budapest, Hungary) with a Zeiss objective (Plan APOchromat 40×; numerical aperture 0.95; ZEISS, Oberkochen, Germany) and a high-resolution color camera (CIS VCC-FC60FR19CL, 4MP, CIS Corporation, Japan). The images were read by using the Pannoramic Viewer software (3D HISTECH Ltd, Budapest, Hungary).

### Confocal imaging

Cells were imaged as previously described (Juin et al., 2014). Cells were imaged with a SP5 confocal microscope (Leica, Leica microsystems GmbH, Wetzlar, Germany) using a ×63/numerical aperture (NA) 1.4 Plan Neofluor objective lens. To prevent contamination between fluorochromes, each channel was imaged sequentially by using the multitrack recording module before merging. *z*-stack pictures were obtained using LAS AF, Leica software. Three-dimensional reconstructions were obtained from *z*-cut pictures, by using Imaris software (Bitplane, Zurich, Switzerland).

## Quantification

### Unr-NRs

We used a macro with ImageJ software that allowed measurement of Unr-NRs number and diameter. Nuclear DNA content was quantified by using total DAPI fluorescence intensity per nucleus using ImageJ. A minimum of 100 cells were counted for each field.

### Statistics

Data are reported as mean±s.d. Significance was measured using two-tailed Student's test ( $P<0.05$ ).

## Electron microscopy

For transmission electron microscopy (TEM), placentas were washed with ice-cold PBS, fixed in 2.5% glutaraldehyde in 0.1 M phosphate buffer pH 7.4 for 2 h at 4°C, and post-fixed in 1% OsO<sub>4</sub> in phosphate buffer for 2 h at room temperature. Tissue blocks (1–2 mm<sup>3</sup>) were then processed following standard procedures. After fixation, tissue blocks corresponding to the embryonic part of the placenta were dehydrated, embedded in Epoxy resin and sectioned through a series of graded ethanol and propylene oxide. Blocks were sectioned at a thickness of 60 nm by using an Leica Ultracut UCT ultramicrotome. Sections were collected onto copper grids, contrasted with 3% uranyl acetate and lead citrate, and examined by using a transmission electronic microscope (HITACHI H7650).

## Ethics approval and consent to participate

This study was performed in accordance with the European Community Standards on the Care and Use of the Animals and was approved by the Animal Care and Use Committee of the University of Bordeaux, France.

## Acknowledgements

We thank Christophe Grosset, Eric Chevet, Hervé Moine, Juan Iovana, David Bernard, Marc Landry, Michel Moenner, Jean-Philippe Merlio and Jean Rosenbaum for helpful discussions. We thank H el ene Boeuf and Violaine Moreau for critical comments on the manuscript. We thank the experimental histopathology platform, US 005 UMS 3427-TBM CORE, a service unit of the CNRS-INSERM and Bordeaux University. We thank Fabrice Cordelieres from the Bordeaux Imaging Center (BIC) for help in fluorescence quantification, and Lucie Geay and Etienne Gontier from the Pole d'Imagerie Electronique of the BIC for transmission electronic microscopy. We are grateful to Dr. Florence Bernex from the R eseau d'Histologie Exp erimentale de Montpellier, for providing us with the murine tissue microarray used in this work.

## Competing interests

The authors declare no competing or financial interests.

## Author contributions

Conceptualization: F.S., P.D., H.J.-S.; Methodology: F.S., A.G., L.A., H.J.-S.; Validation: H.E., H.J.-S.; Formal analysis: F.S., A.G., L.A., H.E., Z.E., H.J.-S.; Investigation: H.J.-S.; Resources: P.C., N.D.-S., L.M., O.B.; Data curation: L.A., H.E.; Writing—original draft: F.S., H.J.-S.; Writing—review & editing: F.S., H.W., H.J.-S.; Visualization: F.S.; Supervision: F.S., H.J.-S.; Project administration: F.S., H.J.-S.; Funding acquisition: F.S., P.D. The last two authors, P.D. and H.J.-S., are both senior authors who contributed equally.

## Funding

This work was supported by INSERM, Bordeaux University and by Grants from the Ligue Nationale contre le Cancer (comit e des Landes), INCA-DGOS-Inserm 6046, Institut National Du Cancer, PLBIO [grant number: 15-135], SIRIC BRIO and ANR [grant number:13-JJC-JSV1-005. A. G. and P. D. were funded by the SIRIC BRIO (Site de Recherche Int egr ee sur le Cancer- Bordeaux) Grant.

## Data availability

All data generated or analyzed during this study are included in this published article (and its supplementary information files). Request for material should be made to the corresponding author.

## Supplementary information

Supplementary information available online at <http://jcs.biologists.org/lookup/doi/10.1242/jcs.198697.supplemental>

## References

- Abaza, I., Coll, O., Patalano, S. and Gebauer, F. (2006). *Drosophila* UNR is required for translational repression of male-specific lethal 2 mRNA during regulation of X-chromosome dosage compensation. *Genes Dev.* **20**, 380–389.
- Anderson, P. and Kedersha, N. (2009). RNA granules: post-transcriptional and epigenetic modulators of gene expression. *Nat. Rev. Mol. Cell Biol.* **10**, 430–436.
- Boussadia, O., Amiot, F., Cases, S., Triqueneaux, G., Jacquemin-Sablon, H. and Dautry, F. (1997). Transcription of *unr* (upstream of N-ras) down-modulates N-ras expression in vivo. *FEBS Lett.* **420**, 20–24.
- Boussadia, O., Niepmann, M., Cr ancier, L., Prats, A.-C., Dautry, F. and Jacquemin-Sablon, H. (2003). Unr is required in vivo for efficient initiation of translation from the internal ribosome entry sites of both rhinovirus and poliovirus. *J. Virol.* **77**, 3353–3359.
- Buchan, J. R. (2014). mRNP granules. Assembly, function, and connections with disease. *RNA Biol.* **11**, 1019–1030.
- Buchan, J. R. and Parker, R. (2009). Eukaryotic stress granules: the ins and outs of translation. *Mol. Cell* **36**, 932–941.
- Copp, A. J. (1995). Death before birth: clues from gene knockouts and mutations. *Trends Genet.* **11**, 87–93.
- David, A., Dolan, B. P., Hickman, H. D., Knowlton, J. J., Clavarino, G., Pierre, P., Bennink, J. R. and Yewdell, J. W. (2012). Nuclear translation visualized by ribosome-bound nascent chain puromycylation. *J. Cell Biol.* **197**, 45–57.
- de Planell-Sagua, M., Rodicio, M. C. and Mourelatos, Z. (2010). Rapid in situ codetection of noncoding RNAs and proteins in cells and formalin-fixed paraffin-embedded tissue sections without protease treatment. *Nat. Protoc.* **5**, 1061–1073.
- Di Leonardo, A., Khan, S. H., Linke, S. P., Greco, V., Seidita, G. and Wahl, G. M. (1997). DNA replication in the presence of mitotic spindle inhibitors in human and mouse fibroblasts lacking either p53 or pRb function. *Cancer Res.* **57**, 1013–1019.
- Dormoy-Raclet, V., Markovits, J., Jacquemin-Sablon, A. and Jacquemin-Sablon, H. (2005). Regulation of Unr expression by 5'- and 3'-untranslated regions of its mRNA through modulation of stability and IRES mediated translation. *RNA Biol.* **2**, e27–e35.
- Dormoy-Raclet, V., Markovits, J., Malato, Y., Huet, S., Lagarde, P., Montaudon, D., Jacquemin-Sablon, A. and Jacquemin-Sablon, H. (2007). Unr, a cytoplasmic RNA-binding protein with cold-shock domains, is involved in control of apoptosis in ES and HuH7 cells. *Oncogene* **26**, 2595–2605.

- Duncan, K., Grskovic, M., Strein, C., Beckmann, K., Niggeweg, R., Abaza, I., Gebauer, F., Wilim, M. and Hentze, M. W. (2006). Sex-lethal imparts a sex-specific function to UNR by recruiting it to the *msl-2* mRNA 3' UTR: translational repression for dosage compensation. *Genes Dev.* **20**, 368–379.
- Echevarria, W., Leite, M. F., Guerra, M. T., Zipfel, W. R. and Nathanson, M. H. (2003). Regulation of calcium signals in the nucleus by a nucleoplasmic reticulum. *Nat. Cell Biol.* **5**, 440–446.
- Elatmani, H., Dormoy-Raclet, V., Dubus, P., Dautry, F., Chazaud, C. and Jacquemin-Sablon, H. (2011). The RNA-binding protein Unr prevents mouse embryonic stem cells differentiation toward the primitive endoderm lineage. *Stem Cells* **29**, 1504–1516.
- Eulalio, A., Behm-Ansmant, I. and Izaurralde, E. (2007). P bodies: at the crossroads of post-transcriptional pathways. *Nat. Rev. Mol. Cell Biol.* **8**, 9–22.
- Fricke, M., Hollinshead, M., White, N. and Vaux, D. (1997). Interphase nuclei of many mammalian cell types contain deep, dynamic, tubular membrane-bound invaginations of the nuclear envelope. *J. Cell Biol.* **136**, 531–544.
- Gehrig, K., Cornell, R. B. and Ridgway, N. D. (2008). Expansion of the nucleoplasmic reticulum requires the coordinated activity of lamins and CTP: phosphocholine cytidyltransferase alpha. *Mol. Biol. Cell* **19**, 237–247.
- Graumann, P. L. and Marahiel, M. A. (1998). A superfamily of proteins that contain the cold-shock domain. *Trends Biochem. Sci.* **23**, 286–290.
- Grosset, C., Chen, C.-Y., Xu, N., Sonenberg, N., Jacquemin-Sablon, H. and Shyu, A.-B. (2000). A mechanism for translationally coupled mRNA turnover: interaction between the poly(A) tail and a c-fos RNA coding determinant via a protein complex. *Cell* **103**, 29–40.
- Hau, P. M., Siu, W. Y., Wong, N., Lai, P. B. S. and Poon, R. Y. C. (2006). Polyploidization increases the sensitivity to DNA-damaging agents in mammalian cells. *FEBS Lett.* **580**, 4727–4736.
- Horos, R. and von Lindern, M. (2012). Molecular mechanisms of pathology and treatment in Diamond Blackfan Anaemia. *Br. J. Haematol.* **159**, 514–527.
- Hosoda, N., Lejeune, F. and Maquat, L. E. (2006). Evidence that poly(A) binding protein C1 binds nuclear pre-mRNA poly(A) tails. *Mol. Cell Biol.* **26**, 3085–3097.
- Hunt, S. L., Hsuan, J. J., Totty, N. and Jackson, R. J. (1999). unr, a cellular cytoplasmic RNA-binding protein with five cold-shock domains, is required for internal initiation of translation of human rhinovirus RNA. *Genes Dev.* **13**, 437–448.
- Ihle, J. N. (2000). The challenges of translating knockout phenotypes into gene function. *Cell* **102**, 131–134.
- Jacquemin-Sablon, H., Triqueneaux, G., Deschamps, S., le Maire, M., Doniger, J. and Dautry, F. (1994). Nucleic acid binding and intracellular localization of unr, a protein with five cold shock domains. *Nucleic Acids Res.* **22**, 2643–2650.
- Jeffers, M., Paciucci, R. and Pellicer, A. (1990). Characterization of unr; a gene closely linked to N-ras. *Nucleic Acids Res.* **18**, 4891–4899.
- Johnson, N., Krebs, M., Boudreau, R., Giorgi, G., LeGros, M. and Larabell, C. (2003). Actin-filled nuclear invaginations indicate degree of cell de-differentiation. *Differentiation* **71**, 414–424.
- Jokhi, V., Ashley, J., Nunnari, J., Noma, A., Ito, N., Wakabayashi-Ito, N., Moore, M. J. and Budnik, V. (2013). Torsin mediates primary envelopment of large ribonucleoprotein granules at the nuclear envelope. *Cell Rep* **3**, 988–995.
- Juin, A., Di Martino, J., Leitinger, B., Henriot, E., Gary, A.-S., Paysan, L., Bomo, J., Baffet, G., Gauthier-Rouvière, C., Rosenbaum, J. et al. (2014). Discoidin domain receptor 1 controls linear invadosome formation via a Cdc42-Tuba pathway. *J. Cell Biol.* **207**, 517–533.
- Katsanou, V., Milatos, S., Yiakoukaki, A., Sgantzis, N., Kotsoni, A., Alexiou, M., Harokopos, V., Aidinis, V., Hemberger, M. and Kontoyiannis, D. L. (2009). The RNA-binding protein Elavl1/HuR is essential for placental branching morphogenesis and embryonic development. *Mol. Cell Biol.* **29**, 2762–2776.
- Kedersha, N. and Anderson, P. (2007). Mammalian stress granules and processing bodies. *Methods Enzymol.* **431**, 61–81.
- Kobayashi, H., Kawauchi, D., Hashimoto, Y., Ogata, T. and Murakami, F. (2013). The control of precerebellar neuron migration by RNA-binding protein Csd1. *Neuroscience* **253**, 292–303.
- Lemay, J.-F., Lemieux, C., St-André, O. and Bachand, F. (2010). Crossing the borders: poly(A)-binding proteins working on both sides of the fence. *RNA Biol.* **7**, 291–295.
- Lerner, R. S. and Nicchitta, C. V. (2006). mRNA translation is compartmentalized to the endoplasmic reticulum following physiological inhibition of cap-dependent translation. *RNA* **12**, 775–789.
- Lin, L., Xu, B. and Rote, N. S. (2000). The cellular mechanism by which the human endogenous retrovirus ERV-3 env gene affects proliferation and differentiation in a human placental trophoblast model. *BeWo. Placenta* **21**, 73–78.
- Litwiniec, A., Gackowska, L., Helmin-Basa, A., Zuryń, A. and Grzanka, A. (2013). Low-dose etoposide-treatment induces endoreplication and cell death accompanied by cytoskeletal alterations in A549 cells: Does the response involve senescence? The possible role of vimentin. *Cancer Cell Int* **13**, 9.
- Liu, Y. and Bodmer, W. F. (2006). Analysis of P53 mutations and their expression in 56 colorectal cancer cell lines. *Proc. Natl. Acad. Sci. USA.* **103**, 976–981.
- Lui, P. P., Kong, S. K., Kwok, T. T. and Lee, C. Y. (1998). The nucleus of HeLa cell contains tubular structures for Ca<sup>2+</sup> signalling. *Biochem. Biophys. Res. Commun.* **247**, 88–93.
- Lu, Z. H., Books, J. T. and Ley, T. J. (2005). YB-1 is important for late-stage embryonic development, optimal cellular stress responses, and the prevention of premature senescence. *Mol. Cell Biol.* **25**, 4625–4637.
- Malhas, A., Goulbourne, C. and Vaux, D. J. (2011). The nucleoplasmic reticulum: form and function. *Trends Cell Biol.* **21**, 362–373.
- Mao, Y. S., Zhang, B. and Spector, D. L. (2011). Biogenesis and function of nuclear bodies. *Trends Genet.* **27**, 295–306.
- Maquat, L. E., Hwang, J., Sato, H. and Tang, Y. (2010). CBP80-promoted mRNP rearrangements during the pioneer round of translation, nonsense-mediated mRNA decay, and thereafter. *Cold Spring Harb. Symp. Quant. Biol.* **75**, 127–134.
- Marth, C., Lang, T., Widschwendter, M., Müller-Holzner, E. and Daxenbichler, G. (1995). Effects of Taxol on choriocarcinoma cells. *Am. J. Obstet. Gynecol.* **173**, 1835–1842.
- Mihailovich, M., Militti, C., Gabaldón, T. and Gebauer, F. (2010). Eukaryotic cold shock domain proteins: highly versatile regulators of gene expression. *BioEssays* **32**, 109–118.
- Mitchell, S. A., Spriggs, K. A., Coldwell, M. J., Jackson, R. J. and Willis, A. E. (2003). The Apaf-1 internal ribosome entry segment attains the correct structural conformation for function via interactions with PTB and unr. *Mol. Cell* **11**, 757–771.
- Negrini, M., Sabbioni, S., Haldar, S., Possati, L., Castagnoli, A., Corallini, A., Barbanti-Brodano, G. and Croce, C. M. (1994). Tumor and growth suppression of breast cancer cells by chromosome 17-associated functions. *Cancer Res.* **54**, 1818–1824.
- Nicolaiew, N., Triqueneaux, G. and Dautry, F. (1991). Organization of the human N-ras locus: characterization of a gene located immediately upstream of N-ras. *Oncogene* **6**, 721–730.
- Patalano, S., Mihailovich, M., Belacortu, Y., Paricio, N. and Gebauer, F. (2009). Dual sex-specific functions of Drosophila Upstream of N-ras in the control of X chromosome dosage compensation. *Development* **136**, 689–698.
- Patel, G. P., Ma, S. and Bag, J. (2005). The autoregulatory translational control element of poly(A)-binding protein mRNA forms a heteromeric ribonucleoprotein complex. *Nucleic Acids Res.* **33**, 7074–7089.
- Rossant, J. and Cross, J. C. (2001). Placental development: lessons from mouse mutants. *Nat. Rev. Genet.* **2**, 538–548.
- Sanders, S. J., Murtha, M. T., Gupta, A. R., Murdoch, J. D., Raubeson, M. J., Willsey, A. J., Ercan-Sencicek, A. G., DiLullo, N. M., Parikshak, N. N., Stein, J. L. et al. (2012). De novo mutations revealed by whole-exome sequencing are strongly associated with autism. *Nature* **485**, 237–241.
- Schoenfelder, K. P. and Fox, D. T. (2015). The expanding implications of polyploidy. *J. Cell Biol.* **209**, 485–491.
- Sheth, U., Pitt, J., Dennis, S. and Priess, J. R. (2010). Perinuclear P granules are the principal sites of mRNA export in adult *C. elegans* germ cells. *Development* **137**, 1305–1314.
- Shibayama, M., Ohno, S., Osaka, T., Sakamoto, R., Tokunaga, A., Nakatake, Y., Sato, M. and Yoshida, N. (2009). Polypyrimidine tract-binding protein is essential for early mouse development and embryonic stem cell proliferation. *FEBS J.* **276**, 6658–6668.
- Speese, S. D., Ashley, J., Jokhi, V., Nunnari, J., Barria, R., Li, Y., Ataman, B., Koon, A., Chang, Y.-T., Li, Q. et al. (2012). Nuclear envelope budding enables large ribonucleoprotein particle export during synaptic Wnt signaling. *Cell* **149**, 832–846.
- Stumpo, D. J., Byrd, N. A., Phillips, R. S., Ghosh, S., Maronpot, R. R., Castranio, T., Meyers, E. N., Mishina, Y. and Blackshear, P. J. (2004). Chorioallantoic fusion defects and embryonic lethality resulting from disruption of Zfp36L1, a gene encoding a CCH tandem zinc finger protein of the Tristetraprolin family. *Mol. Cell Biol.* **24**, 6445–6455.
- Triqueneaux, G., Velten, M., Franzone, P., Dautry, F. and Jacquemin-Sablon, H. (1999). RNA binding specificity of Unr, a protein with five cold shock domains. *Nucleic Acids Res.* **27**, 1926–1934.
- Unsworth, H., Raguz, S., Edwards, H. J., Higgins, C. F. and Yague, E. (2010). mRNA escape from stress granule sequestration is dictated by localization to the endoplasmic reticulum. *FASEB J.* **24**, 3370–3380.
- Weil, T. T., Parton, R. M., Herpers, B., Soetaert, J., Veenendaal, T., Xanthakis, D., Dobbie, I. M., Halstead, J. M., Hayashi, R., Rabouille, C. et al. (2012). Drosophila patterning is established by differential association of mRNAs with P bodies. *Nat. Cell Biol.* **14**, 1305–1313.
- Wolffe, A. P. (1994). Structural and functional properties of the evolutionarily ancient Y-box family of nucleic acid binding proteins. *BioEssays* **16**, 245–251.
- Wurth, L., Papsaikas, P., Olmeda, D., Bley, N., Calvo, G. T., Guerrero, S., Cerezo-Wallis, D., Martinez-Useros, J., Garcia-Fernandez, M., Hüttelmaier, S. et al. (2016). UNR/CSDE1 Drives a Post-transcriptional Program to Promote Melanoma Invasion and Metastasis. *Cancer Cell* **30**, 694–707.
- Xia, K., Guo, H., Hu, Z., Xun, G., Zuo, L., Peng, Y., Wang, K., He, Y., Xiong, Z., Sun, L. et al. (2014). Common genetic variants on 1p13.2 associate with risk of autism. *Mol. Psychiatry* **19**, 1212–1219.
- Yasuda, K., Zhang, H., Loisel, D., Haystead, T., Macara, I. G. and Mili, S. (2013). The RNA-binding protein Fus directs translation of localized mRNAs in APC-RNP granules. *J. Cell Biol.* **203**, 737–746.